CREEP BEHAVIOR OF Ti-6Al-4V FROM 450°C TO 600°C

Lavinia BADEA[1], Martin SURAND[2], Jacques RUAU[3], Bernard VIGUIER[4]

We present in this paper the creep behavior of Ti-6Al-4V from 450°C to 600°C under applied stress from 100 MPa to 500 MPa. Creep behavior is studied analyzing creep damage after tests and calculating stress exponent (n) and activation energy (Q). Operating creep deformation mechanisms characterization is possible by analyzing crept microstructure by TEM. A comparison of n and Q values with values from literature and a correlation with TEM micrographs will lead us to a discussion about operating creep deformation mechanisms.

Keywords: Ti-6Al-4V, creep, titanium alloy, Norton coefficient, activation energy

1. Introduction

Due to their very good specific mechanical properties and corrosion resistance, titanium alloys are currently widely used in aerospace industry. The most commonly used titanium alloy for aircraft's engine applications is Ti-6Al-4V. This alloy is used for numerous structural parts of airplanes, as well as in the low temperature parts of the turbine aerospace engines [1]. The mechanical behavior of Ti-6Al-4V has been investigated over a large range of temperature, from very low temperature for cryogenic applications [2, 3] to very high temperature for forming conditions [4] around 950°C. Industrial applications usually limit Ti-6Al-4V use to 400°C. The objectives of the present research are to explore the possible application range of this alloy, in terms of temperature and stress, above 400°C. Tensile properties have been characterized over a large range of temperature, from room temperature to 600°C [5]. This paper will focus on creep behavior of Ti-6Al-4V from 450°C to 600°C.

2. Experimental details

The studied material comes from a hot-forged billet of Ti-6Al-4V in the α+β phase field. Chemical composition is presented in Table 1. Thermo

[1] Master Student, State Faculty of Pitesti, Pitesti, Romania, e-mail: badealavinia.florina@yahoo.com
[2] PhD student, Institut Carnot CIRIMAT, ENSIACET INP Université de Toulouse, France
[3] DGA Techniques Aéronautiques, DMP, DMTP, Toulouse, France
[4] Prof., Institut Carnot CIRIMAT, ENSIACET INP Université de Toulouse, France, e-mail: bernard.viguier@ensiacet.fr

mechanical treatment of the alloy implies duplex microstructure with equiaxed α grains with average size about 20 μm and lamellar grains which are α laths in a β matrix. An optical micrograph of the microstructure is shown in Fig. 1.

Table 1

Chemical composition of the Ti-6Al-4V alloy

Chemical element	Al	V	Impurities	Ti
% in weight	6.44	3.87	<0.4	89.29

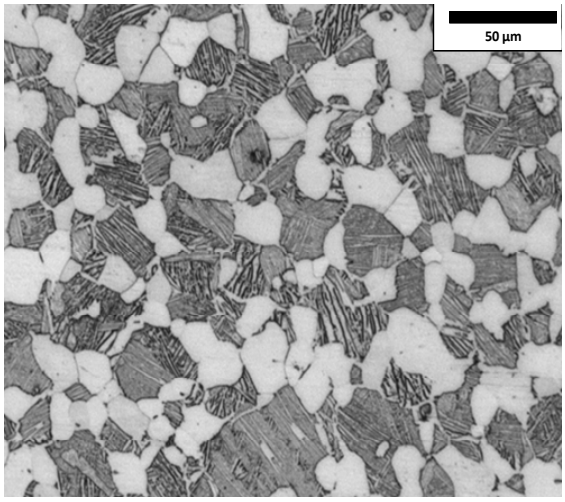

Fig. 1. Optical micrograph of as-received Ti-6Al-4V microstructure

Tensile testing was performed on a servo-hydraulic MTS 810 testing machine under imposed displacement velocity of $5x10^{-3}$ $mm.s^{-1}$ which corresponds to a strain rate of $1.6x10^{-4}$ s^{-1}. Basic tensile mechanical properties of the studied alloy are summarized in Table 2, at 450°C and 600°C. YS is the 0.2% yield stress, UTS is the ultimate tensile stress and RS the rupture strain.

Table 2

Basic tensile mechanical properties of Ti-6Al-4V

Temperature	YS (MPa)	UTS (MPa)	RS (%)
450°C	480	650	17
600°C	330	400	45

Creep tests have been performed from 450°C to 600°C under a range of stress from 100 MPa to 600 MPa on several creep frame (dead weight and screw driven machine) under imposed load. Ti-6Al-4V cylindrical specimens of total length 45 mm and diameter gage 4.5 mm were machined from the billet. Temperature and stress values imposed for creep tests conditions are presented in

Fig. 2 together with UTS and YS evolution versus temperature. For each creep test a r parameter is defined as a ratio of the applied stress during creep over the YS of the alloy during imposed strain rate tensile testing at the same temperature (1). This r parameter indicates stress level of the creep test. For some tests the creep stress is sometimes higher than the YS.

$$r = \left. \frac{\sigma_{creep}}{YS\,(\dot{\varepsilon} = 1.6\,10^{-4}\,s^{-1})} \right)_T \tag{1}$$

Fracture surface of crept specimens have been analyzed in scanning electron microscopy (SEM) using a LEO 435-VP. Creep test damage under fracture surface is analyzed by optical microscopy using an Olympus PGM3 microscope equipped with a 500D Nikon camera. Operating deformation mechanisms is characterized by analyzing deformed microstructure by a JEOL JEM 2010 transmission electron microscope equipped with a lanthanum hexaboride (LaB_6) source. Analyzed samples are extracted from crept specimens and observed in a plan perpendicular to load axis.

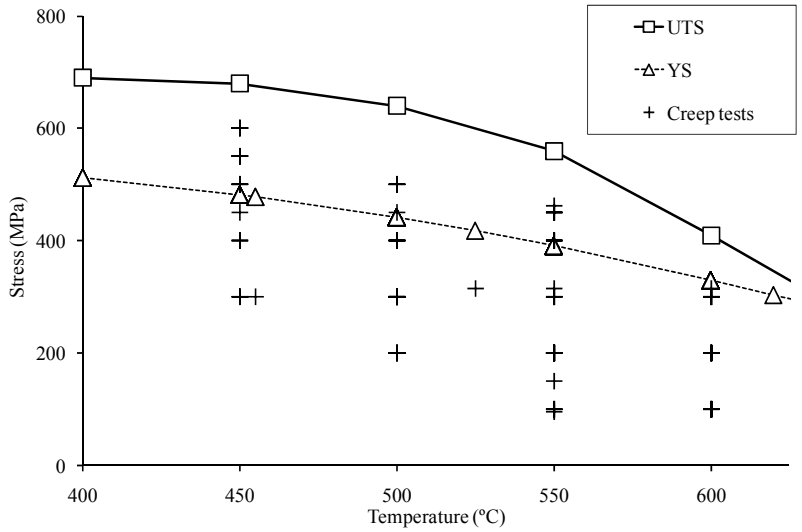

Fig. 2. Map of temperature and stress conditions for creep tests together with YS and UTS evolution as measured during imposed strain rate tensile tests at $\dot{\varepsilon} = 1.6 \times 10^{-4} s^{-1}$

3. Results

Measured creep curves from 450°C to 600°C show typical high temperature creep behavior. Representative creep curves of T-64 creep behavior at 450°C under 400 MPa and at 600°C under 200 MPa are respectively plotted in Fig. 3 and Fig. 4. For both conditions creep curves present three stages: primary,

secondary (steady-state) and tertiary. The primary creep strain is quite limited as compared to steady-state and tertiary strain and moreover primary strain decreases with increasing temperature. The sample deformation mainly occurs during steady-state and the amount of steady state creep strain increases with stress and/or temperature increase. A comparison between Fig. 3 and Fig. 4 shows a decreasing creep resistance versus temperature because even if stress level decreases while temperature increases steady-state creep strain rate increases and rupture happens earlier.

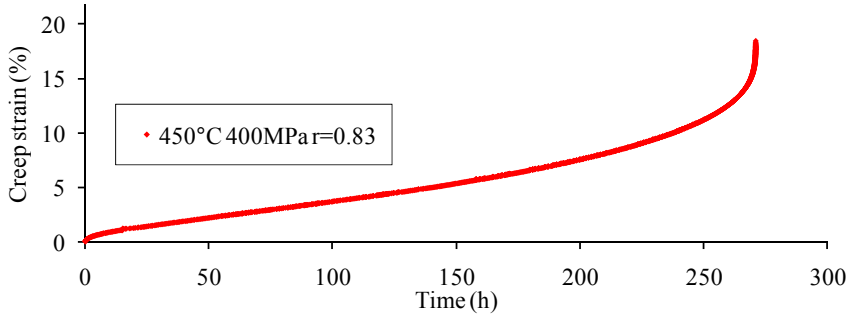

Fig. 3. Ti-6Al-4V creep curve at 450°C under 400 MPa (r = 0.83)

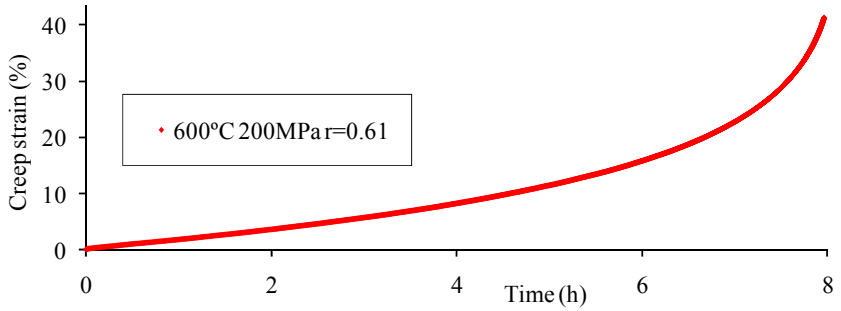

Fig. 4. Ti-6Al-4V creep curve at 600°C under 200 MPa (r = 0.61)

Fig. 6 show micrographs of specimens crept respectively at 450°C under 450 MPa and at 600°C under 100 MPa. Figs. 5a and 6a are the fracture surfaces of crept specimens observed by SEM. For both creep conditions, fracture surfaces exhibit ductile rupture characteristics, with a more pronounced necking, deeper voids and larger void diameters for the higher temperature test as compared to the lower temperature. Optical micrographs presented in Figs. 5b and 6b show creep damage beneath fracture surfaces for both specimens. Creep damage is characterized by cavities at grain boundaries due to vacancies clustering. Cavity sizes and quantities increase with increasing temperature and decreasing stress since those conditions favor diffusion mechanisms and vacancies accumulation.

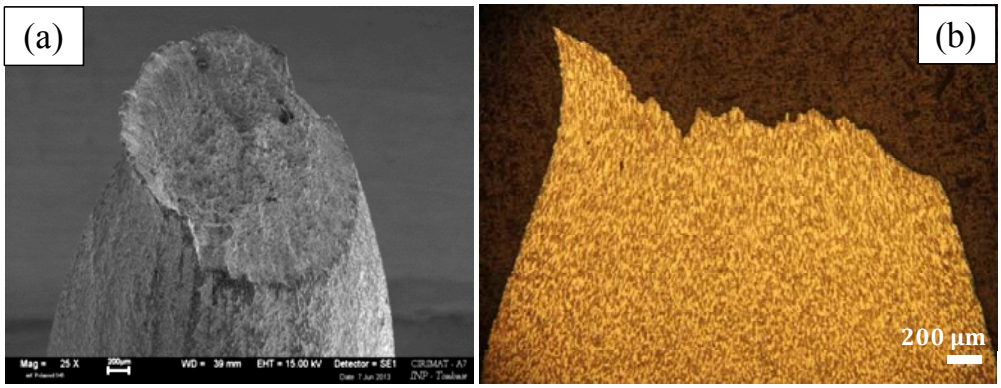

Fig. 5. SEM and optical microscope micrograph at 450°C under 450 MPa, the rupture time is t_R = 135 h.

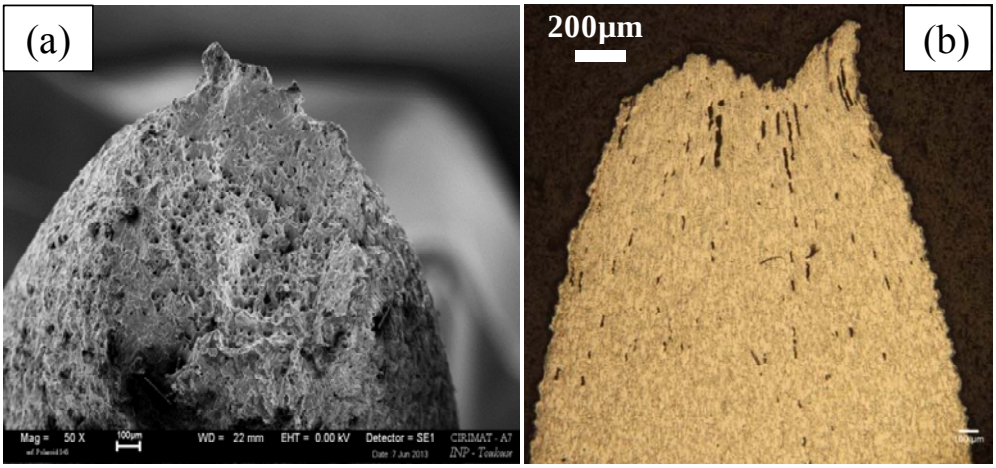

Fig. 6. SEM and optical microscope micrograph at 600°C under 100 MPa, the rupture time is t_R = 180 h.

Most of creep life is dominated by a constant creep rate that depends on temperature and stress. The steady-state creep rate is usually described by a power law for stress dependence and an Arrhenius law for temperature dependence, as written in equation (2).

$$\dot{\varepsilon} = A\sigma^n \exp\left(-\frac{Q}{RT}\right) \tag{2}$$

$\dot{\varepsilon}$ (s^{-1}) is the steady state creep strain rate, A is a constant depending on the material properties, σ (MPa) is the applied stress during creep test, n is the stress exponent, Q (J/mol) is the activation energy, R is the universal constant of gases and T (K) the temperature at which creep test was performed. In this general equation (2), the stress exponent (n) and the activation energy (Q) characterize the activated deformation mechanism.

At 450°C, 500°C, 550°C and 600°C evolution of steady-state creep strain rate versus stress is shown in Fig. 7. In this log-log plot it appears that experimental points align along two different segments for each temperature depending on the creep stress level. Calculated stress exponent values are reported in Table 3. For low stresses (≤ 0.8xYS), values of stress exponent around 5 are found whereas for higher stresses (> 0.8xYS), values higher than 10 are found. A similar result was reported by Barboza et al. at 500°C and 600°C for Ti-6Al-4V [6] who estimated a stress exponent n = 4.2 for 600°C tests with relatively low stress (r values from 025 to 085) while they obtained n = 8.89 at 500°C for higher stress (r values from 055 to 1).

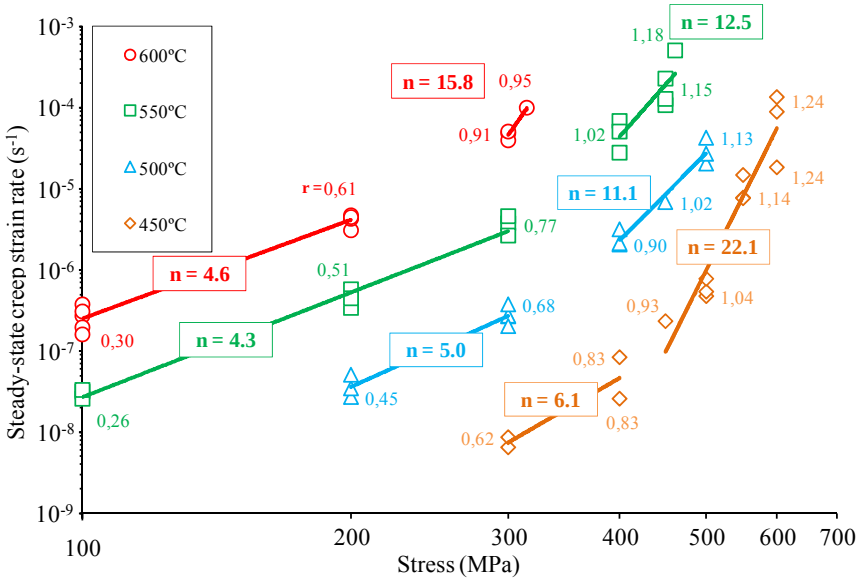

Fig. 7. Dependence of steady-state creep rate on applied stress at 500°C and 600°C. The YS ratios (r value) corresponding to the creep loads are noted beside the experimental points. The framed numbers correspond to the Norton stress exponents.

Table 3

Stress exponent values for temperatures from 450°C to 600°C

Temperature (°C)	450	500	550	600
n (r ≤ 0.9)	6.1	5.0	4.3	4.6
n (r > 0.9)	22.1	11.1	12.5	15.8

Under stresses from 100 MPa to 500 MPa, the variation of steady-state creep strain rate versus the creep temperature is plotted in Fig. 8. In the range of applied stress and temperature, creep activation energy values from Fig. 8 are reported in Table 4. There is a large range of activation energy values from 251 kJ/mol to 326 kJ/mol. Barboza et al. have measured an activation energy of 319 kJ/mol from 500°C to 600°C under 291 MPa [6].

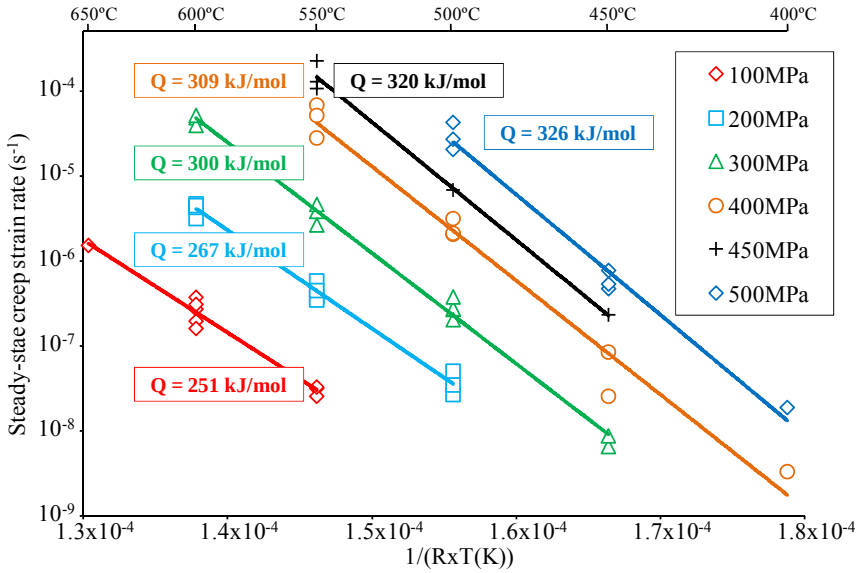

Fig. 8. Dependence of steady-state creep rate on temperature at an applied stress between 100 MPa and 600 MPa

Table 4

Creep activation energy values for stresses from 100 MPa to 500 MPa

Stress (MPa)	100	200	300	400	450	500
Activation energy (kJ/mol)	251	267	300	309	320	326

In order to characterize the operating deformation mechanisms, interrupted creep tests have been conducted at 600°C and 200MPa up to 0.86% strain. Thin foils were then extracted and examined by TEM. The observation of dislocations with several diffraction vectors has shown a predominance of dislocations with <a> Burgers vector.

Fig. 9 shows two TEM micrographs of the same area imaged using two different diffraction vectors. Figs. 9a and 9b respectively correspond to the $10\bar{1}0$ and the $\bar{1}10\bar{1}$ diffraction vectors. In Fig. 9a dislocations with a $a/3\,[\bar{1}\bar{1}20]$ Burgers vector are observed to be gliding on prismatic plans. Fig. 9b presents dislocations with a $a/3\,[\bar{1}2\bar{1}0]$ Burgers vector exhibiting more complex line

morphology with open loops and none planar structure as indicated by small arrows. These observations agree with recent literature about deformation mechanisms in titanium alloys [7]. These dislocation shapes are usually due to dislocation climb which can be correlated to typical stress exponent and activation energy values measured for diffusion mechanisms.

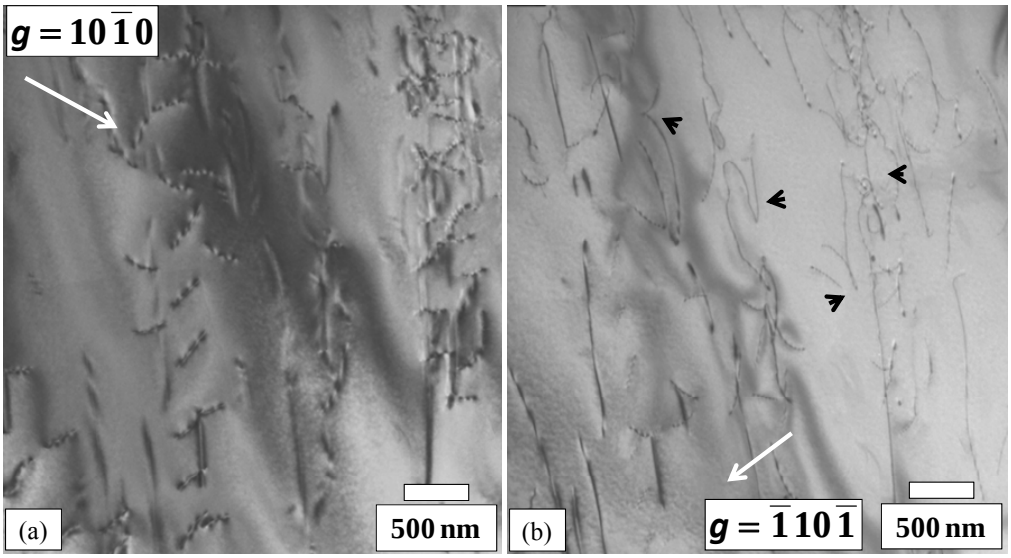

Fig. 9. TEM micrographs for two diffraction vectors after 0.86% creep deformation at 600°C under 200 MPa

4. Discussion

The high temperature creep results on Ti-6Al-4V alloy that are reported in the present study can be compared to results obtained on similar or different Ti alloys as reported in the literature. Various values are reported in the literature for the stress exponent in the secondary creep rate expression given in equation (2). The lowest values, $n \approx 1$, are reported for lower stress levels associated to Harper-Dorn creep regime [8]. For higher stress levels the stress exponent can either be in the range 4-6 [8-12] or reach quite unusual high values $n > 15$ [13]. In a recent review on Ti alloys prospective [14] Banerjee and Williams indicate that these results can be rationalized and the highest exponent values bring back to about 4-5 by the use of a threshold stress [13]. However the physical meaning of this threshold stress is not always obvious and it is not very clear why such high exponent values are observed or not [14]. In the present study we observed that

for a given temperature the usual values of stress exponents are associated to creep tests conducted at stress level corresponding to $r < 0.9$ whereas the highest n values are associated to creep tests conducted under higher stress level ($r > 0.9$).

Dislocation microstructure observations after creep tests corresponding to $n \approx 4\text{-}6$ values reveal the presence of cusped screw dislocation with $1/3\langle\bar{1}\bar{1}20\rangle$ Burgers vectors. Those observations are very similar to the ones by Viswanathan et al. [8] who reported <a> dislocations pinned along screw direction and bowed between pinning points which are tall jogs. In this stress and temperature regime it can be concluded that creep rate is controlled by <a> type dislocation climb. For higher stress levels, the stress exponent is not really meaningful; this regime is qualified of power law break-down and may be associated to dislocation glide and climb processes such as the ones activated during the alloy plasticity.

From the creep tests reported in this study, it has been possible to extract activation energy values. Creep activation energy is usually compared to activation energy for self-diffusion and for alloy elements diffusion. In literature, titanium self-diffusion activation energy values of 123 kJ/mol [15], 150 kJ/mol [16], 241 kJ/mol [17] and 303 kJ/mol [18] are reported and measured by radiotracer. For diffusion of Al in titanium, a value of 329 kJ/mol is measured by Koppers et al. [19]. Miller et al. report for oxygen diffusion values of 68 kJ/mol [20], 109 kJ/mol [21], 140 kJ/mol [22] under moderate temperature during long time. Previously reported results have shown a large range of creep activation energy values from 180 kJ/mol to 350 kJ/mol for many stress conditions and many kind of titanium alloys [8-10, 12, 23-26]. Above 400°C, Rosen and Rottem measured an activation energy value of 188 kJ/mol for Ti-64 [26] which is in agreement with Li et al. reporting a value of 185 kJ/mol [24] in the same range of temperature. For alpha titanium Malakondaiah and Rama Rao measured a value of 104 kJ/mol for temperature below 700°C. Rosen and Rottem associated the creep mechanism operating with titanium self-diffusion. Malakondaiah and Rama Rao localize titanium diffusion in grain boundaries. Measured creep activation energies in our study are included in the range of values given by literature. We believe that the activation energy associated to the low stress level ($r < 0.9$), that is values ranging from 250 to 300 kJ/mol are the more reliable. This range of activation energy fits quite well with titanium self-diffusion values, confirming the role of dislocation climb during creep. For higher stress level equation (2) is no more relevant since we are within the power law break-down regime and the measured energy is just an apparent activation energy which is not necessarily related to a single process.

5. Conclusions

Creep behavior of Ti-6Al-4V has been characterized in the temperature range 450°C to 600°C. Quite few creep results are reported in the literature in this temperature range in contrast with lower temperature studied for cryogenic applications or higher temperature for forming conditions for which data are much more numerous.

In the whole temperature range explored in the present study, Ti-6Al-4V alloy shows a typical high temperature creep behavior with a relatively low primary stage, an extended steady state deformation that is responsible of the large secondary creep strain and a progressive tertiary creep leading to rupture. Creep resistance of Ti-6Al-4V decreases with temperature increase.

The evolution of steady state creep rate with stress and temperature has been analyzed. There is a transition in stress exponent values with stress. For stress lower than 0.9xYS, steady-state creep strain rate dependency with stress follows a power law close to diffusion model ($n \approx 4$-5). For stress higher than 0.9xYS, a power law breakdown domain is observed. Activation energy values measured in this temperature domain for the lower stresses are similar to the ones reported in literature and can be related to self-diffusion activation energies in titanium. TEM observations of dislocation microstructure reveal the activation of dislocations <a> type Burgers vector mainly of screw character but exhibiting numerous cusps and non-planar configurations. We deduced that, in the investigated temperature domain 450-600°C and moderate stress level, the creep deformation of Ti-64 is mainly controlled by the climbing process of <a> dislocations.

R E F E R E N C E S

[1]. *R. R. Boyer*, "An overview on the use of titanium in the aerospace industry", in Materials Science and Engineering: A, **vol. 213**, no. 1–2, 1996, p. 103

[2]. *J. Luo, M. Li, W. Yu and H. Li*, "The variation of strain rate sensitivity exponent and strain hardening exponent in isothermal compression of Ti-6Al-4V alloy", in Materials & Design, **vol. 31**, no. 2, 2010, p. 741

[3]. *B. C. Odegard and A. W. Thompson*, "Low temperature creep of Ti-6Al-4V", in Metallurgical Transactions A, **vol. 5**, no. 1974, p. 1207

[4]. *Y. Niu, M. Li, H. Hou, Y. Wang and Y. Lin*, "High-Temperature Deformation Behaviour of Ti-6Al-4V Alloy without and with Hydrogenation Content of 0.27 wt.%", in ASM International, **vol. JMEPEG**, no. 19, 2010, p. 59

[5]. *M. Surand, B. Viguier, E. Herny and J. Ruau*, Expanding the application range of Ti-6Al-4V alloy, MS&T 2012, **vol. 2**, Pittsburgh, 2012, p. 1518

[6]. *M. J. R. Barboza, C. M. Neto and C. R. M. Silva*, "Creep mechanisms and physical modeling for Ti-6Al-4V", in Materials Science & Engineering, **vol. A**, no. 369, 2004, p. 201

[7]. *J. H. Moon, S. Karthikeyan, B. M. Morrow, S. P. Fox and M. J. Mills*, "High-temperature creep behaviour and microstructure analysis of binary Ti-6Al alloys with trace amounts of Ni", in Materials Science and Engineering, **vol. A**, no. 510-511, 2009, p. 35

[8]. *G. B. Viswanathan, S. Karthikeyan, R. W. Hayes and M. J. Mills*, "Creep behaviour of Ti-6Al-2Sn-4Zr-2Mo : II. Mechanisms of deformation", in Acta Materialia, **vol. 50**, no. 0, 2002, p. 4965

[9]. *M. Es-Souni*, "Primary, secondary and anelastic creep of a high temperature near alpha-Ti alloy Ti6242Si", in Materials Characterization, **vol. 45**, no. 11, 2000, p. 153

[10]. *M. Es-Souni*, "Creep behaviour and creep microstructures of a high-temperature titanium alloy Ti-5.8Al-4.0Sn-3.5Zr-0.7Nb-0.35Si-0.06C (Timetal 834) Part I. Primary and steady-state creep", in Materials Characterization, **vol. 46**, no. 5, 2001, p. 365

[11]. *J. H. Zhu, P. K. Liaw, J. M. Corum and H. H. McCoy*, "High-Temperature Mechanical Behavior of Ti-6Al-4V Alloy and TiC/Ti-6Al-4V Composite", in Metallurgical and Materials Transactions A, **vol. 30**, no. 6, 1999, p. 1569

[12]. *D. A. P. Reis, C. R. M. Silva, M. C. A. Nono, M. J. R. Barboza, F. P. Neto and E. A. C. Perez*, "Effect of environment on the creep behavior of Ti-6Al-4V alloy", in Materials Science and Engineering A, **vol. 399**, no. 1-2, 2005, p. 276

[13]. *W. J. Evans and G. F. Harrison*, "Power law steady state creep in α/β titanium alloys", in Journal of Materials Science, **vol. 18**, no. 11, 1983, p. 3449

[14]. *D. Banerjee and J. C. Williams*, "Perspectives on Titanium Science and Technology", in Acta Materialia, **vol. 61**, no. 3, 2013, p. 844

[15]. *C. M. Libanati and S. F. Dyment*, "Autodifusion de titanio alfa", in Acta Metallurgica, **vol. 11**, no. 11, 1963, p. 1263

[16]. *F. Dyment and C. M. Libanati*, "Self-Diffusion of Ti, Zr, and Hf in their HCP Phases, and Diffusion of Nb(95) in HCP Zr", in Journal of Materials Science, **vol. 3**, no. 4, 1968, p. 349

[17]. *G. Malakondaiah, N. Prasad and P. Rama Rao*, "On the evaluation of activation energy for viscous creep through temperature change tests", in Scripta Metallurgica, **vol. 16**, no. 4, 1982, p. 421

[18]. *M. Köppers, D. Derdau, M. Friesel and C. Herzig*, "Self-diffusion and group III (Al, Ga, In) solute diffusion in hcp titanium", in Defect and Diffusion Forum, **vol. 143**, no. 1997, p. 43

[19]. *M. Köppers, C. Herzig and M. Friesel*, "Intrinsic self-diffusion and substitutional Al diffusion in alpha-Ti", in Acta Materialia, **vol. 45**, no. 10, 1997, p. 4181

[20]. *R. P. Elliot*, Study of Advanced Flight-Vehicle Power-Utilization Systems, ASD-TDR-62-561, General Dynamics, 1962, p. 44

[21]. *E. A. Gulbransen and K. F. Andrew*, "Kinetics of the reactions of Titanium with O-2, N-2 and H-2", in Transactions of the American Institute of Mining and Metallurgical Engineers, **vol. 185**, no. 10, 1949, p. 741

[22]. *N. P. Roe, H. R. Palmer and W. R. Opie*, in Transactions of ASM, **vol. 52**, no. , 1960, p. 191

[23]. *J. P. Quast and C. J. Boehlert*, "Comparaison of the Microstructure, Tensile, and Creep Behavior for Ti-24Al-17Nb-0.66Mo (Atomic Percent) and Ti-24Al-17Nb-2.3Mo (Atomic Percent) Alloys", in Metallurgical and Materials Transactions A, **vol. A**, no. 38, 2007, p. 529

[24]. *X. Li, T. Sugui, B. Xianyu and C. Liqing*, "Creep properties and effect factors of hot continuous rolled Ti–6Al–4V alloy", in Materials Science and Engineering: A, **vol. 529**, no. 0, 2011, p. 452

[25]. *F. Tang, S. Nakazawa and M. Hagiwara*, "Transient creep of Ti-Al-Nb alloys", in Materials Science and Engineering, **vol. A**, no. 325, 2002, p. 194

[26]. *A. Rosen and A. Rottem*, "The effect of high temperature exposure on the creep ressitance of Ti-6Al-4V alloy", in Materials Science and Engineering, **vol. 22**, no. 1, 1976, p. 23